Supporting Information for

In Situ Healing of Compromised Membranes via Polyethyleneimine-Functionalized Silica Microparticles

Sang-Ryoung Kim, Bezawit A. Getachew, and Jae-Hong Kim*

Department of Chemical and Environmental Engineering Yale University, New Haven, Connecticut 06511, United States

*Corresponding Author

Phone: +1-203-432-4386; fax: +1-203-432-4387; e-mail: Jaehong.kim@yale.edu

Supporting Information includes the following figures, as cross referenced through the main article:

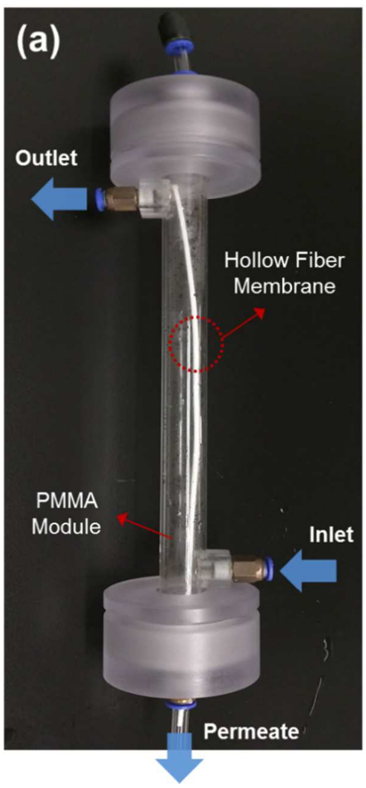

(b)

Cleanfil® Membrane Specifications	
Company	Kolon Industry Inc.
Material	Polyvinylidene fluoride
Type	Braid-reinforced hollow fiber
Pore size	0.1 µm
Outer diameter	2.0 mm
Inner diameter	0.8 mm

Figure S 1. (a) Image of the pressurized membrane module. The custom module was prepared for hollow fiber membrane filtration test using a transparent poly (methyl methacrylate) (PMMA) shell (length = 300 mm, Inner diameter = 12 mm, Outer diameter = 18 mm). (b) Specifications of Cleanfil® membrane that was used for filtration experiments in this study.

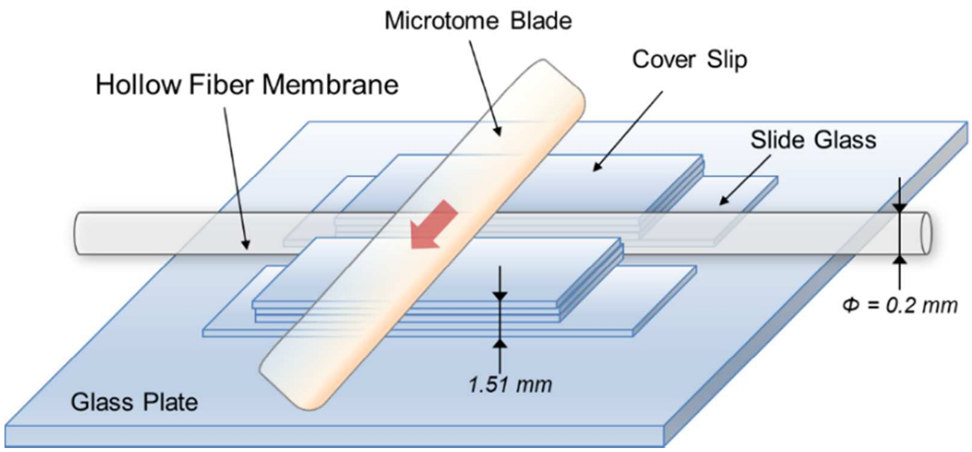

Figure S 2. Membrane damaging scheme using customized microtome device. The hollow fiber membrane (Φ =0.2 mm) was damaged between glass supports of the same height (1.51 mm) to induce damages in a reproducible manner.

Observation of FITC-Labeled Silica Microparticles Deposition by using CLSM. To confirm deposition of silica microparticles, we used CLSM imaging (Nikon C2, Japan, 488 and 561 nm solid-state laser). Synthesized SiO_2@FITC MPs suspension was injected into the 2 L dispensing vessel at a concentration of 0.25%. The procedure for the deposition experiments was the same as the *in situ* healing process, as described in Figure 2. The power of the laser lines and detector gain values were constant throughout the experiment, and sample membranes were observed with a ×10 objective lens. The observed images covered an area of 1100 × 1100 μm^2 with a resolution of 512 × 512 pixels. The images were analyzed with a Nikon software (NIS-Elements or IMARIS, Bitplane, Switzerland). The z-section image stack (slice thickness: 10 μm) was reconstructed using IMARIS software (Bitplane AG, Switzerland). Image Structure Analyzer in three-dimensions (ISA-2) was used to quantitatively analyze the particle deposition structure in terms of its volume and thickness.

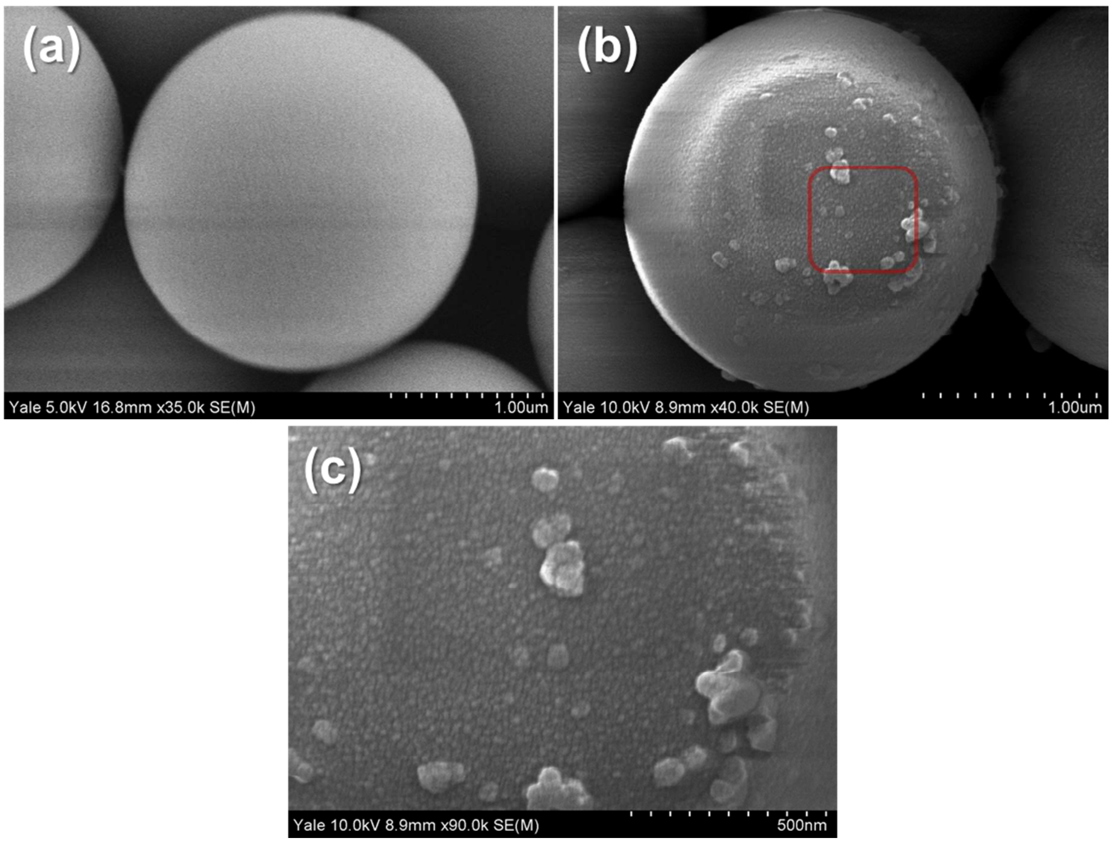

Figure S 3. SEM images of (a) pristine SiO_2 MPs, (b) SiO_2@PEI MPs, and (c) SiO_2@PEI MPs surface with higher magnification.

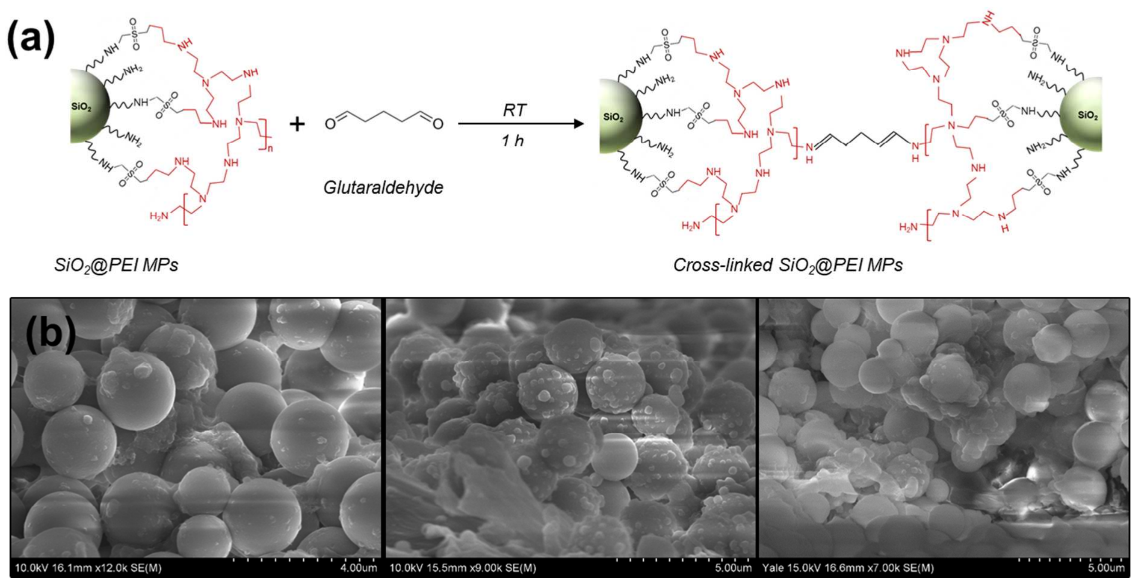

Figure S 4. (a) Reaction scheme of the formation of cross-linked SiO_2@PEI MPs via coupling with glutaraldehyde. (b) Representative SEM images of cross-linked SiO_2@PEI MPs in damage site after *in situ* healing.

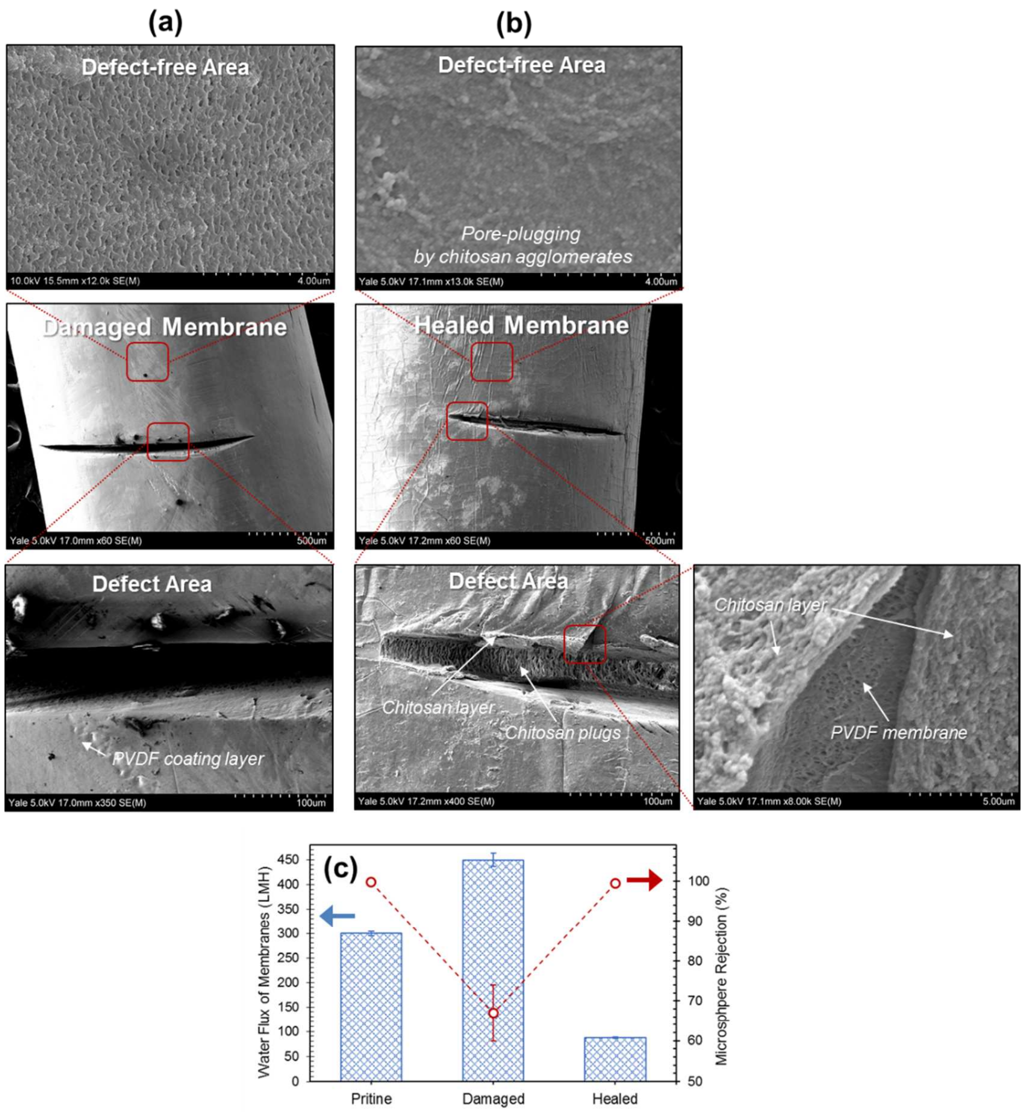

Figure S 5. Representative SEM images of (a) damaged membrane and (b) *in situ* healed membrane by using chitosan agglomerates. (c) Water flux and rejection recovery of *in situ* healed membrane by using chitosan agglomerates. Chitosan *in situ* healing was performed using the following steps: i) Membrane damaging with microtome blade device; ii) filtration of chitosan agglomerate suspension (prepared to 0.02 wt% chitosan at pH 7.0) for 10 min; iii) 1st DI water flushing for 60 min; iv) injection and filtration of 1 wt% glutaraldehyde solution for 10 min; v) cross-linking reaction for 60 min; vi) 2nd DI water flushing for 60 min. The operating condition was set to 34 kPa and 1.0 L/min of cross-flow rate. The chitosan for this experiments was purchased from Sigma-Aldrich (50-190 kDa of molecular weight, USA).

Calculation of Flow Rate through the Damage Site.

From the experimental result at 34 kPa operating pressure,

$$J_p\ (J_{pristine\ membranes}) \approx 301\ \text{LMH}\ (\text{L/m}^2\cdot\text{h}) = Q_p / A$$

$$J_c\ (J_{compromised\ membranes}) \approx 441\ \text{LMH} = Q_c / A$$

where,

A = effective filtration area of pristine membrane = 17.6 cm^2 = 1.76×10^{-3} m^2

A_d = defect area of damaged membrane (0.0168% of total membrane area)

≈ 1244 µm (length) × 88 µm (width) = 109472 μm^2 = 1.09×10^{-7} m^2

Thus,

∴ Q_p = flow rate through a pristine membrane

$= 301\ \text{L/m}^2\cdot\text{h} \times 10^{-3}\ \text{m}^3/\text{L} \times 1.76 \times 10^{-3}\ \text{m}^2 = 5.29 \times 10^{-4}\ \text{m}^3/\text{h} = 1.47 \times 10^{-7}\ \text{m}^3/\text{s}$

∴ Q_c = flow rate through a compromised membrane

$= 412\ \text{L/m}^2\cdot\text{h} \times 10^{-3}\ \text{m}^3/\text{L} \times 1.76 \times 10^{-3}\ \text{m}^2 = 7.25 \times 10^{-4}\ \text{m}^3/\text{h} = 2.16 \times 10^{-7}\ \text{m}^3/\text{s}$

Flow rate through the compromised membrane (Q_c) is the sum of the flow through defect-free (i.e. intact) membrane area (Q_{df}) and the flow through defect area (Q_d):

$$Q_c = Q_{df} + Q_d = [Q_p \times (\text{A} - \text{A}_\text{d})/\text{A}] + Q_d$$

$$2.16 \times 10^{-7}\ \text{m}^3/\text{s} = [1.47 \times 10^{-7}\ \text{m}^3/\text{s} \times \{1 - (1.09 \times 10^{-7})/(1.76 \times 10^{-3})\}] + Q_d$$

$$\therefore\ Q_d = 6.84 \times 10^{-8}\ \text{m}^3/\text{s}$$

Therefore, the specific flux through the defect area (J_d) can be calculated from Q_d using the defect area of damaged membrane (A_d), as follows:

$$\therefore J_d = \frac{6.84 \times\ 10^{-8}\ m^3/s \times 1000\ L \times 3600\ s}{1\ m^3 \times 1.09 \times 10^{-7} m^2 \times 1\ h} = 2.25 \times 10^6\ L/m^2 \cdot h\ \ (LMH)$$

The experimental flux through the defect area under various operating condition (28, 34, 48, and 72 kPa) has been calculated using the same method and is shown in Figure 2. This is in line with the previous studies that show the increase of 10 - 1000% in surface permeability due to the damage in a polymeric membrane.[1-5]

Table S 1. Estimation of flow through the defect-free and defect area under various operating conditions.

Operating conditions		Experimental results			
	Cross-flow Rate (Q_{cf}, L/min)	Permeate of pristine membrane ($L \cdot m^{-2} \cdot h^{-1}$)	Permeate of compromised membrane ($L \cdot m^{-2} \cdot h^{-1}$)	Flow through defect-free area (Q_{df}, m^3/s)	Flow through defect area (Q_d, m^3/s)
Set 1	0.5	177 ± 19.8	288 ± 20.1	8.65×10^{-5}	5.43×10^{-8}
Set 2	1	301 ± 15.2	441 ± 21.7	1.47×10^{-7}	6.84×10^{-8}
Set 3	1.5	420 ± 33.4	597 ± 41.8	2.05×10^{-7}	8.65×10^{-8}
Set 4	2	530 ± 12.4	872 ± 77.2	2.59×10^{-7}	1.67×10^{-7}

Table S 2. SiO_2@PEI MPs transportation forces associated with drag and axial directions. The values were calculated based on the method above with Table S1.

Operating conditions			Axial component		Drag component	
	Operating Pressure (kPa)	Cross-flow Rate (Q_{cf}, L/min)	Cross-flow velocity (V_{cf}, m/s)	Specific flux through the membrane module (J_{cf}, $L \cdot m^{-2} \cdot h^{-1}$)	Specific flux through the defect-free site (J_{df}, $L \cdot m^{-2} \cdot h^{-1}$)	Specific flux through the defect site (J_d, $L \cdot m^{-2} \cdot h^{-1}$)
Set 1	28	0.5	3.79×10^{-2}	1.36×10^{5}	1.77×10^{2}	1.78×10^{6}
Set 2	34	1	7.58×10^{-2}	2.73×10^{5}	3.01×10^{2}	2.25×10^{6}
Set 3	48	1.5	1.14×10^{-1}	4.09×10^{5}	4.20×10^{2}	2.84×10^{6}
Set 4	72	2	1.52×10^{-1}	5.46×10^{5}	5.30×10^{2}	5.49×10^{6}

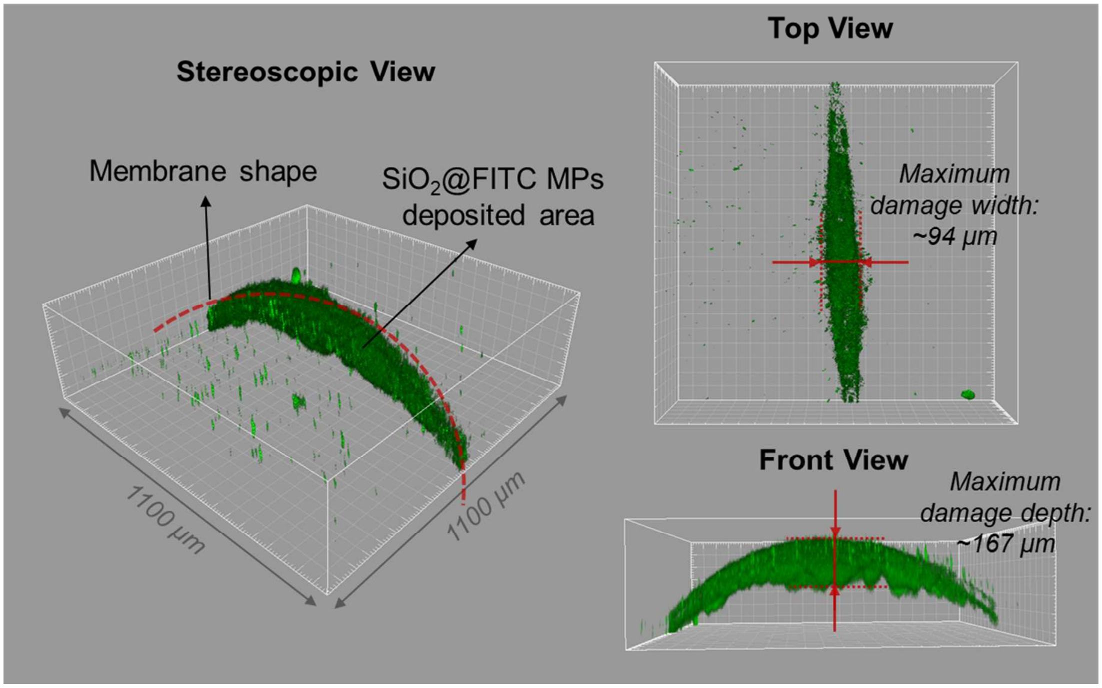

Figure S 6. Observation of SiO_2@FITC MPs deposition on damage area by using CLSM. The image was obtained using a 10× objective lens with depth scanning at 10 µm resolution. The three-dimensional images were reconstructed using IMARIS. The filtration system was operated with a cross-flow rate of 1.0 ± 0.07 L/min, operating pressure of 34 ± 1.7 kPa, and at 20 °C). Specific *in situ* healing process: SiO_2@PEI MPs: 5 min; 1st flushing: 10 min; glutaraldehyde: 10 min; cross-linking reaction: 60 min; 2nd flushing: 30 min.

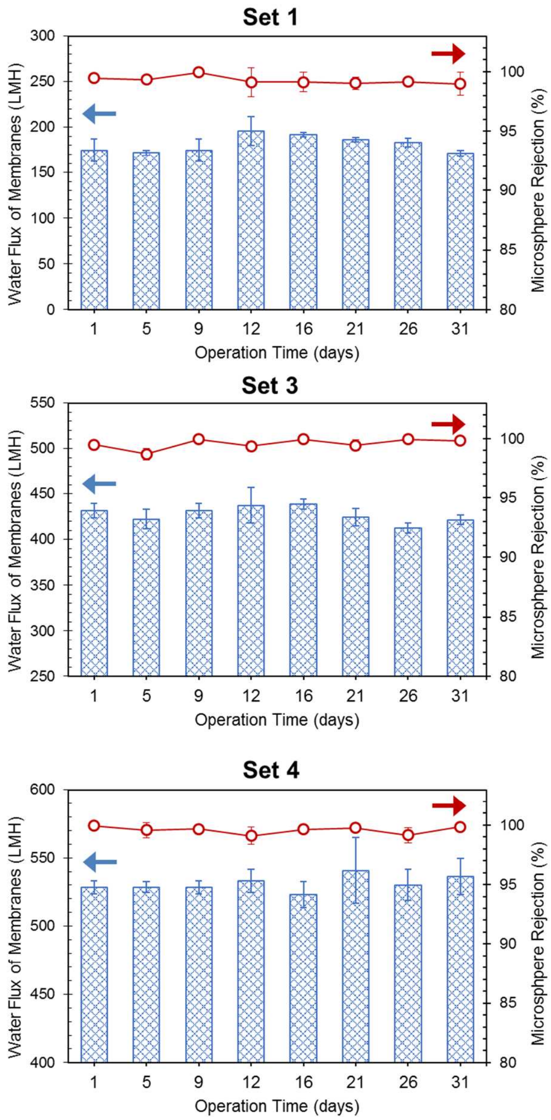

Figure S 7. Long-term stability of *in situ* healed membrane with periodic chemical washing. Operating condition of experimental sets (pressure (kPa), cross-flow rate (L/min)) as follows: set 1 (28, 0.5); set 3 (48, 1.5); set 4 (72, 2.0). All membranes were chemically cleaned by soaking 100 mg/L of sodium hypochlorite for 1h every day. Particle rejection and water flux were just measured after chemical cleaning.

Reference

1. Getachew, B. A.; Kim, S. R.; Kim, J. H., Self-healing hydrogel pore-filled water filtration membranes. *Environ. Sci. Technol.* **2017,** *51*, (2), 905-913.

2. Kim, S. R.; Getachew, B. A.; Kim, J. H., Toward microvascular network-embedded self-healing membranes. *J. Membr. Sci.* **2017,** *531*, 94-102.

3. Kim, S. R.; Getachew, B. A.; Park, S.-J.; Kwon, O. S.; Ryu, W. H.; Taylor, A. D.; Bae, J.; Kim, J. H., Toward microcapsule-embedded self-healing membranes. *Environ. Sci. Technolo. Lett.* **2016,** *3*, (5), 216-221.

4. Lee, S. J.; Getachew, B. A.; Kim, J. H., Restoring the virus removal capability of damaged hollow fiber membranes via chitosan-based in situ healing. *J. Membr. Sci.* **2016,** *497*, 387-393.

5. Zaribaf, B. H.; Lee, S. J.; Kim, J. H.; Park, P. K.; Kim, J. H., Toward in situ healing of compromised polymeric membranes. *Environ. Sci. Technol. Lett.* **2014,** *1*, (1), 113-116.